

Cross-plane phonon transport in thin films

D. P. Sellan,¹ J. E. Turney,² A. J. H. McGaughey,^{2,a)} and C. H. Amon^{1,2}

¹Department of Mechanical & Industrial Engineering, University of Toronto, Toronto, Ontario M5S 3G8, Canada

²Department of Mechanical Engineering, Carnegie Mellon University, Pittsburgh, Pennsylvania 15213, USA

(Received 18 June 2010; accepted 20 October 2010; published online 9 December 2010)

We predict the cross-plane phonon thermal conductivity of Stillinger-Weber silicon thin films as thin as 17.4 nm using the lattice Boltzmann method. The thin films are modeled using bulk phonon properties obtained from harmonic and anharmonic lattice dynamics calculations. We use this approach, which considers all of the phonons in the first Brillouin-zone, to assess the suitability of common assumptions. Specifically, we assess the validity of: (i) neglecting the contributions of optical modes, (ii) the isotropic approximation, (iii) assuming an averaged bulk mean-free path, and (iv) the Matthiessen rule. Because the frequency-dependent contributions to thermal conductivity change as the film thickness is reduced, assumptions that are valid for bulk are not necessarily valid for thin films. © 2010 American Institute of Physics. [doi:10.1063/1.3517158]

I. INTRODUCTION

Thermal transport in microstructured and nanostructured materials can be significantly different than in bulk. As dimensions are reduced, boundary effects become significant and properties predicted for the bulk phase (e.g., thermal conductivity, phonon relaxation times) may not be suitable for modeling thermal transport. One example is the semiconductor thin film, which is common in microprocessors, solid-state memory, and semiconductor light-emitting diodes.^{1–3} The reduced thermal conductivity of thin films limits their ability to effectively remove waste heat, which is critical to device operation and reliability.^{2–4}

In this work, we use the phonon Boltzmann transport equation (BTE) under the relaxation-time approximation to predict (i) the bulk thermal conductivity of Stillinger-Weber (SW) silicon and (ii) the cross-plane thermal conductivity of SW silicon thin films as thin as 17.4 nm, all at a temperature of 300 K. We analyzed the in-plane thermal conductivity in a previous report.⁵ The accuracy of the BTE predictions depends on the accuracy of the phonon properties required as input. Given an interatomic potential that describes the atomic interactions, mode-dependent specific heats and group velocities can be predicted using harmonic lattice dynamics calculations.^{6,7} The required relaxation times can be predicted from molecular dynamics (MD) simulation^{8,9} or anharmonic lattice dynamics calculations.^{7,10} MD simulation and anharmonic lattice dynamics calculations, the latter of which naturally includes quantum effects and is used here, are computationally expensive and can be challenging to implement. As such, we also investigate the suitability of four approximations commonly made to reduce the computational effort. First, we assess the validity of neglecting the contributions of optical phonons. Second, the isotropic approximation, where the phonon properties of one crystalline direction are assumed to be representative of the entire Brillouin-zone. Third, the Gray approximation, where the en-

tire Brillouin-zone is represented by a single phonon velocity and relaxation time. Finally, the Matthiessen rule, which assumes that different scattering mechanisms are independent. By investigating these approximations, we will (i) determine when they can be used to predict the phonon properties and thermal conductivity of bulk systems without introducing significant error, and (ii) understand how their validity changes as system lengths are reduced from bulk to the nanometer scale.

To perform the required calculations, we use a hierarchical procedure (described in Sec. II A) that uses the BTE (Secs. II B and II C) and lattice dynamics calculations (Sec. II D) to predict the bulk and cross-plane thin film thermal conductivities. In Sec. III, we present the thermal conductivity predictions and examine the role of optical phonons, the isotropic and Gray approximations, and the suitability of the Matthiessen rule for combining the effects of different scattering mechanisms. We show that because the frequency-dependent contributions to thermal conductivity change as the film thickness is reduced, approximations that are valid for bulk are not necessarily valid for thin films.

II. COMPUTATIONAL TOOLS

A. Overview of the hierarchical procedure

The thermal conductivity of a solid, \mathbf{k} , is a second-order tensor empirically defined by the Fourier law

$$\mathbf{q} = -\mathbf{k} \nabla T, \quad (1)$$

where \mathbf{q} is the heat flux vector and ∇T is the temperature gradient in the material. At the atomic level, the thermal conductivity of a semiconductor is related to the transport of phonons (i.e., quanta of lattice vibration). We model phonon transport using the hierarchical procedure shown in Fig. 1 and describe in detail in Secs. II B–II D. Interatomic force constants, which are the derivatives of a system's potential energy with respect to the positions of its constituent atoms, are first calculated from an interatomic potential energy function. The force constants are then used in harmonic and an-

^{a)}Electronic mail: mcgaughey@cmu.edu.

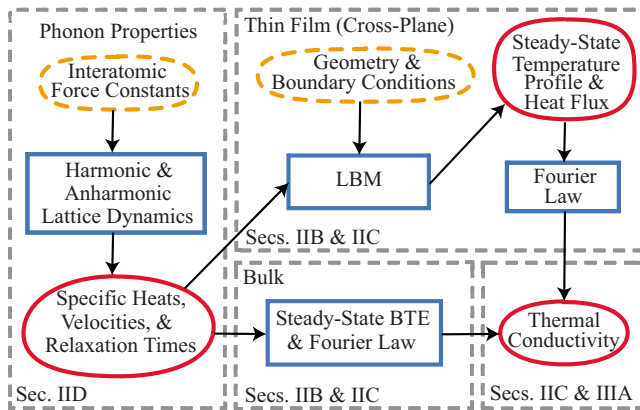


FIG. 1. (Color online) Flow chart of the hierarchical procedure for predicting the phonon thermal conductivity of bulk and thin films using lattice dynamics calculations and the BTE. The theoretical/computational tools are in boxes and their inputs and outputs are in ovals.

harmonic lattice dynamics calculations to predict mode-dependent phonon specific heats, group velocities, and relaxation times.^{7,11}

For bulk systems, these phonon properties are used in a steady-state solution of the BTE that is combined with Eq. (1) to predict the thermal conductivity. For thin films, the lattice Boltzmann method (LBM) is used to discretize the BTE and then solve it numerically for the phonon occupation numbers in a system with a specified geometry and boundary conditions.^{12,13} The steady-state phonon occupation numbers are then used to calculate the temperature profile and heat flux. From these values, Eq. (1) is used to calculate the thermal conductivity. Although previous works have used the LBM to model phonon transport in thin films, these studies assumed forms for the frequency dependence of phonon relaxation times that require fitting parameters^{13–18} and/or were limited to isotropic material properties.¹⁹ Our approach does not rely on the isotropic approximation or any fitting parameters. Methods other than the LBM, such as the equation of radiative phonon transport²⁰ and the discrete ordinate method,²¹ have also been used to solve the BTE. These methods, however, are often used with a single group velocity and an averaged bulk relaxation time, which, while making them fast to execute, can introduce significant error (see Sec. III C).

B. Boltzmann transport equation

The time-dependent BTE for each phonon mode is given by²²

$$\frac{\partial f(\boldsymbol{\kappa}, \nu)}{\partial t} + \mathbf{v}_g(\boldsymbol{\kappa}, \nu) \cdot \nabla f(\boldsymbol{\kappa}, \nu) = \left[\frac{\partial f(\boldsymbol{\kappa}, \nu)}{\partial t} \right]_{\text{coll}}, \quad (2)$$

where $f(\boldsymbol{\kappa}, \nu)$ is the phonon occupation number. Each phonon mode is identified by its wave vector, $\boldsymbol{\kappa}$, and dispersion branch, ν . The phonon group velocity vector, $\mathbf{v}_g(\boldsymbol{\kappa}, \nu)$, is

$$\mathbf{v}_g(\boldsymbol{\kappa}, \nu) = \frac{\partial \omega(\boldsymbol{\kappa}, \nu)}{\partial \boldsymbol{\kappa}}, \quad (3)$$

where $\omega(\boldsymbol{\kappa}, \nu)$ is the phonon frequency. The left hand side of Eq. (2) describes the diffusion of a system of noninteracting

phonons. The term on the right hand side is the collision operator and serves to reestablish equilibrium through phonon scattering. The phonon modes are coupled through the collision operator.

The overriding challenge in solving the BTE is modeling the collision operator. Although methods have been developed to evaluate it directly,^{11,23,24} here we use the relaxation-time approximation to make solving the BTE more tractable.^{25,26} Under this approximation, phonon transport is described by a set of mode-dependent relaxation times, $\tau(\boldsymbol{\kappa}, \nu)$, defined as the average time between scattering events. We assume that the crystal contains no defects, no free electrons, and no internal interfaces so that $\tau(\boldsymbol{\kappa}, \nu)$ is equal to the relaxation time associated with phonon-phonon scattering, $\tau_{p-p}(\boldsymbol{\kappa}, \nu)$. The collision term is modeled as

$$\left[\frac{\partial f(\boldsymbol{\kappa}, \nu)}{\partial t} \right]_{\text{coll}} = \frac{f^{\text{BE}}(\boldsymbol{\kappa}, \nu) - f(\boldsymbol{\kappa}, \nu)}{\tau_{p-p}(\boldsymbol{\kappa}, \nu)}, \quad (4)$$

where $f^{\text{BE}}(\boldsymbol{\kappa}, \nu)$ is the Bose-Einstein (equilibrium) distribution function

$$f^{\text{BE}}(\boldsymbol{\kappa}, \nu) = \frac{1}{e^{\chi} - 1}, \quad (5)$$

and $\chi \equiv \hbar \omega(\boldsymbol{\kappa}, \nu) / k_B T$, \hbar is the Planck constant divided by 2π , k_B is the Boltzmann constant, and T is the absolute temperature. Combining Eqs. (2) and (4) yields the BTE under the relaxation-time approximation

$$\frac{\partial f(\boldsymbol{\kappa}, \nu)}{\partial t} + \mathbf{v}_g(\boldsymbol{\kappa}, \nu) \cdot \nabla f(\boldsymbol{\kappa}, \nu) = \frac{f^{\text{BE}}(\boldsymbol{\kappa}, \nu) - f(\boldsymbol{\kappa}, \nu)}{\tau_{p-p}(\boldsymbol{\kappa}, \nu)}. \quad (6)$$

Using a first-principles approach to predict the bulk thermal conductivity of silicon and germanium, Ward and Broido found that the relaxation-time approximation introduces 5%–10% error for temperatures between 100 and 800 K.²⁴

C. Bulk and lattice Boltzmann method solutions to the Boltzmann transport equation

For bulk crystals, the steady-state solution of Eq. (6) can be combined with the Fourier law to develop an expression for the z component of the thermal conductivity tensor^{12,22}

$$k_z = \sum_{\nu} \sum_{\boldsymbol{\kappa}} c_{ph}(\boldsymbol{\kappa}, \nu) v_{g,z}^2(\boldsymbol{\kappa}, \nu) \tau_{p-p}(\boldsymbol{\kappa}, \nu). \quad (7)$$

Here, the phonon specific heat, $c_{ph}(\boldsymbol{\kappa}, \nu)$, is^{12,22}

$$c_{ph}(\boldsymbol{\kappa}, \nu) = \frac{\hbar \omega(\boldsymbol{\kappa}, \nu)}{V} \frac{\partial f^{\text{BE}}(\boldsymbol{\kappa}, \nu)}{\partial T} = \frac{k_B \chi^2}{V} \frac{e^{\chi}}{[e^{\chi} - 1]^2}, \quad (8)$$

where V is the volume of the lattice dynamics computational cell (see Sec. II D), and $v_{g,z}(\boldsymbol{\kappa}, \nu)$ is the z component of the group velocity vector (i.e., along the [001] direction).

To evaluate the thermal conductivity of a thin film using Eq. (7), a correction to the phonon-phonon relaxation times must be made to account for phonon-boundary scattering (e.g., by using the Matthiessen rule, see Sec. III D). We have chosen to use the LBM to solve Eq. (6) numerically and thus do not need to invoke the Matthiessen rule. In the LBM, the temporal-and spatial-variations in the phonon occupation numbers are predicted by solving Eq. (6) numerically.

Consider a thin film oriented such that the cross-plane direction and thermal gradient are along the z direction. For this one-dimensional system, $\nabla f(\kappa, \nu) = \partial f(\kappa, \nu) / \partial z$ and $v_g(\kappa, \nu) = v_{g,z}(\kappa, \nu)$ in Eq. (6). The system is infinite in the x and y (in-plane) directions. For each phonon mode (κ, ν) we solve Eq. (6) by using a first-order discretization in time and space. We then define a time step/lattice spacing relationship such that each phonon mode travels between adjacent nodes in a mode-dependent time step $[\Delta t(\kappa, \nu) = \Delta z / v_{g,z}(\kappa, \nu)]$. This procedure yields the phonon lattice Boltzmann equation

$$f[z + \Delta z, t + \Delta t(\kappa, \nu)] = \left[1 - \frac{\Delta z}{v_{g,z}(\kappa, \nu) \tau_{p-p}(\kappa, \nu)} \right] f[z, t] + \frac{\Delta z}{v_{g,z}(\kappa, \nu) \tau_{p-p}(\kappa, \nu)} f^{\text{BE}}[z, t]. \quad (9)$$

In our procedure for predicting thin film thermal conductivity, phonon scattering is modeled using a two-step process. First, phonons are coupled in the prediction of $\tau_{p-p}(\kappa, \nu)$ (see Sec. II D). Second, during the LBM simulation the phonons exchange energy through the collision operator. As the system evolves in time, a fraction $[\Delta t(\kappa, \nu) / \tau_{p-p}(\kappa, \nu) = \Delta z / v_{g,z}(\kappa, \nu) \tau_{p-p}(\kappa, \nu)]$ of the energy in phonon mode (κ, ν) is redistributed into the equilibrium distribution at every internal node at every time step.

To achieve mesh-independent thermal conductivity predictions in our LBM simulations, we use $\Delta z = \Lambda_{\min}/10$, where Λ_{\min} is the smallest phonon mean-free path (MFP) in the system. The phonon MFP, $\Lambda(\kappa, \nu) = v_{g,z}(\kappa, \nu) \tau_{p-p}(\kappa, \nu)$, is the average distance a phonon travels before it scatters. To prevent the node density from approaching infinity (i.e., if the group velocity or MFP approach zero, which can occur at the Brillouin-zone boundaries), phonons with group velocities less than 25 m/s are neglected, resulting in $\Delta z = 0.1$ nm. As expected, neglecting these small group velocity modes does not significantly affect the thermal conductivity prediction. Their effect on scattering, however, is still included in the prediction of τ_{p-p} .

Since the phonon distribution at each node does not represent an equilibrium distribution, temperature cannot be calculated directly. We define the node temperature by equating the local energy density (i.e., the energy associated with each node) of the nonequilibrium distribution with that of an equilibrium distribution, Eq. (5), where temperature is defined. The local energy density at a node is

$$E_{\text{node}} = \frac{1}{V} \sum_{\nu} \sum_{\kappa} \hbar \omega(\kappa, \nu) [f_L(\kappa, \nu) + f_R(\kappa, \nu)], \quad (10)$$

where L and R denote the left and right propagation directions.²⁷ Because we are using a small temperature difference to impose the heat flux, the nonequilibrium distributions in the film are close to equilibrium and this approximation does not introduce significant error.

Fixed temperature boundary conditions are imposed by using the Bose–Einstein distribution to calculate the phonon occupations numbers corresponding to the desired temperature. This boundary condition ensures that all phonons scatter diffusely when they interact with the system boundaries (i.e., into all directions). The hot and cold boundaries of the

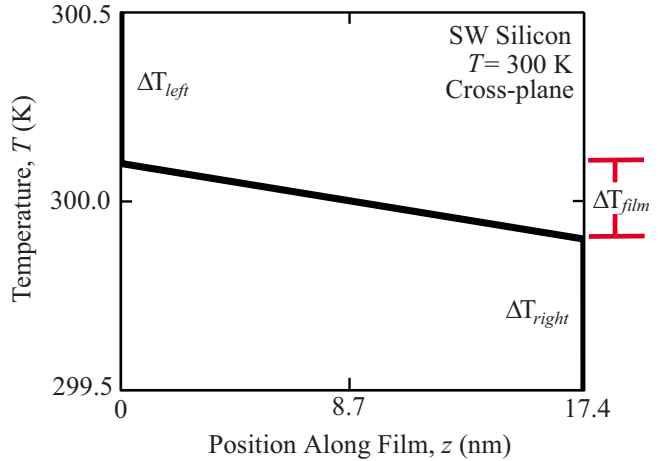


FIG. 2. (Color online) Subcontinuum temperature profile across a 17.4 nm SW silicon thin film predicted using our hierarchical method.

thin film are set to temperatures of 300.5 and 299.5 K, resulting in a temperature difference of 1 K and an average temperature of 300 K. All phonon properties are calculated at a temperature of 300 K. Details related to our LBM methodology are available elsewhere.^{28,29}

The use of completely diffuse boundaries is based on the idea that the reconstruction of free silicon surfaces disrupts phonons traveling in the cross-plane direction. Similarly, for thin films bounded by an amorphous material (e.g., a silicon thin film bounded by amorphous silica layers), we believe that the transition from a crystalline to an amorphous material presents a large disruption to the phonon propagation and will diffusely scatter the majority of incident phonons.

We predict the effective cross-plane thermal conductivity, $k_z(L_z)$, of our thin films using a one-dimensional form of the Fourier Law

$$k_z(L_z) = \frac{q_z L_z}{\Delta T_{\text{left}} + \Delta T_{\text{film}} + \Delta T_{\text{right}}}, \quad (11)$$

where q_z is the z component of the heat flux vector in the thin film ($q_x = q_y = 0$)

$$q_z = \frac{1}{V} \sum_{\nu} \sum_{\kappa} v_{g,z}(\kappa, \nu) \hbar \omega(\kappa, \nu) [f_L(\kappa, \nu) - f_R(\kappa, \nu)], \quad (12)$$

and L_z is the film thickness.²⁷ The temperature differences ΔT_{left} , ΔT_{film} , and ΔT_{right} , are calculated from the steady-state temperature profile, which is shown in Fig. 2 for the 17.4 nm thick film. Of particular interest are the temperature discontinuities at the boundaries (ΔT_{left} and ΔT_{right}), which indicate that some modes travel ballistically. If all modes travel ballistically, then $dT/dz = 0$ and $\Delta T_{\text{left}} = \Delta T_{\text{right}} = 0.5$ K. Such discontinuities are negligible in bulk systems (i.e., $\Delta T_{\text{right}}, \Delta T_{\text{left}} \rightarrow 0$ as $L_z \rightarrow \infty$) and are not predicted using continuum-based analysis techniques. Ballistic transport occurs when the film thickness is comparable to or smaller than the MFP of a phonon mode. In this ballistic (subcontinuum) regime, phonons travel from one side of the film to the other without scattering. It follows from Eq. (7) that these ballistic modes will contribute less to thermal conductivity than they would in a bulk system, as their MFPs are effectively re-

duced to the system length. Thermal conductivity is thus a length-dependent property when ballistic effects are present.

D. Predicting phonon properties using lattice dynamics calculations

To predict the phonon properties required to parameterize Eqs. (7) and (9) [$c_{ph}(\boldsymbol{\kappa}, \nu)$, $v_{g,z}(\boldsymbol{\kappa}, \nu)$, and $\tau_{p-p}(\boldsymbol{\kappa}, \nu)$], we use harmonic and anharmonic lattice dynamics calculations.^{6,7,10} Because we are using a small temperature difference to impose the heat flux, we predict the phonon properties at the average temperature. The lattice dynamics calculations are thus a one-time computational cost. The mode-dependent phonon properties are computed on a $N_0 \times N_0 \times N_0$ grid of wave vectors, making the total number of unit cells equal to $N_0 N_0 N_0$. To achieve size-independent bulk thermal conductivity predictions, we used $N_0 = 10$ and a conventional (i.e., eight atom, simple-cubic) unit cell to generate 55 566 modes in the first Brillouin-zone.

The phonon properties predicted from our lattice dynamics calculations are for bulk systems and naturally include quantum effects. Using harmonic lattice dynamics calculations, Turney *et al.*⁵ found that SW silicon thin films thicker than 17.4 nm have a bulklike density of states. Based on this result, the smallest film thickness we investigate is 17.4 nm, where we expect that the bulk phonon properties can be combined with a suitable boundary scattering model to accurately model the thermal transport.

The atomic interactions in a harmonic lattice dynamics calculation are described by the second-order derivatives of the interatomic potential with respect to the equilibrium positions (i.e., the harmonic force constants). These force constants can be used to determine the natural frequencies of vibration, $\omega(\boldsymbol{\kappa}, \nu)$, of the phonon modes in the crystal. The slope of the corresponding dispersion curves [i.e., $\omega(\boldsymbol{\kappa}, \nu)$] plotted versus $\boldsymbol{\kappa}$, shown in Fig. 3(a) for SW silicon] is then used to predict the group velocities, as defined by Eq. (3).

We apply periodic boundary conditions to our lattice dynamics simulation cell and consider no defects, no free electrons, and no internal interfaces. As such, the only source of intrinsic phonon scattering is the anharmonic interactions between phonon modes. We obtain the phonon-phonon relaxation times, $\tau_{p-p}(\boldsymbol{\kappa}, \nu)$, using anharmonic lattice dynamics calculations, where the third-and fourth-order derivatives of the interatomic potential are used as a perturbation to the harmonic phonon modes.^{6,7} The phonon-phonon relaxation times predicted for SW silicon at a temperature of 300 K are shown in Fig. 3(b). The largest relaxation times are associated with acoustic modes located near the Brillouin-zone center (i.e., $\boldsymbol{\kappa}, \omega=0$), where they approach infinity in an infinite system (i.e., bulk translation).¹²

Lattice dynamics calculations are valid at low temperatures, where the atomic displacements are small compared to the atomic spacing. As temperature increases, the atomic displacements increase and the contributions of the neglected fifth-and higher-order anharmonic terms in the interatomic potential become important. Turney *et al.*⁷ suggest that reasonable predictions of relaxation times and thermal conductivity can be made using lattice dynamics calculations up to

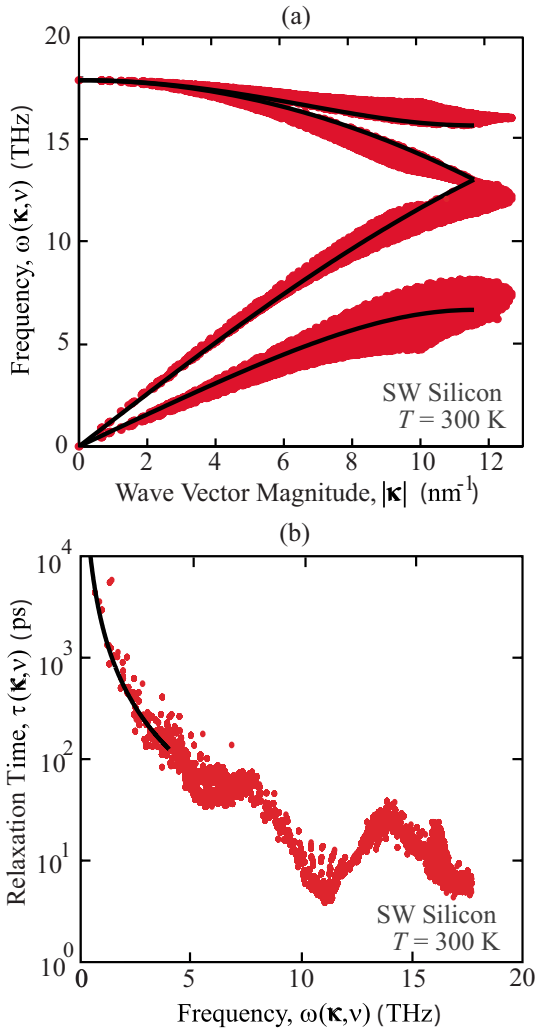


FIG. 3. (Color online) (a) Frequency dependence on wave vector magnitude, $|\boldsymbol{\kappa}|$, for the entire Brillouin-zone of SW silicon at a temperature of 300 K. Dispersion curves corresponding to the [001] direction are shown as solid lines. (b) Phonon relaxation-time dependence on frequency for SW silicon at a temperature of 300 K. Near the Brillouin-zone center, the relaxation times are reasonably represented by $\tau=A/\omega^2$ (solid line) (Ref. 36), where A is a constant calculated for this data to be 2×10^{15} 1/s.

half of the Debye temperature. Here, we consider SW silicon at a temperature of 300 K, which is less than half of its Debye temperature, 710 K.³⁰ Details of our lattice dynamics calculations are provided by Turney and co-workers.^{5,7,31}

III. ANALYZING THE RESULTS AND ASSESSING COMMON ASSUMPTIONS

A. Thermal conductivity predictions

The cross-plane thin film thermal conductivities of SW silicon predicted using the LBM and all the phonons in the first Brillouin-zone are plotted in Fig. 4 (normalized by the bulk value) and listed in Table I (for selected film thicknesses). The lattice dynamics-predicted and experimental bulk silicon thermal conductivities are 574 and 165 W/m K.³² The large difference between these two results is due primarily to the use of the SW potential and, to a lesser degree, the approximations made in the lattice dynam-

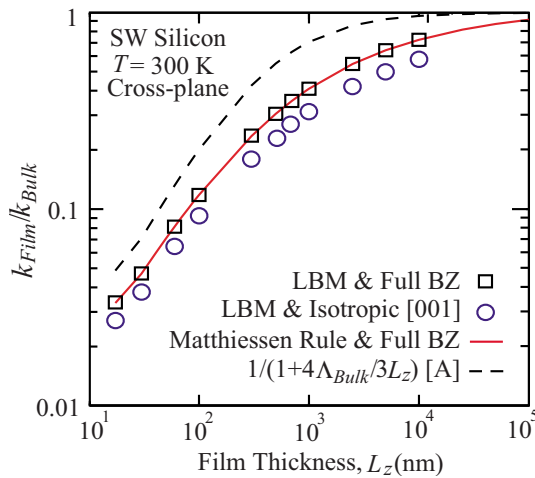


FIG. 4. (Color online) Cross-plane thin film thermal conductivity normalized by the bulk value. We consider phonons from the full Brillouin-zone (squares) and the isotropic approximation (circles). The cross-plane thermal conductivity found using the Matthiessen rule (solid line) and a simplified model (dashed line, see Sec. III C) are also plotted. [A] corresponds to Ref. 20.

ics techniques.³¹ Experimental cross-plane thermal conductivity measurements for silicon thin films are not available.

As shown in Fig. 4, the thermal conductivity increases monotonically to the bulk value as the system length increases. We take the full Brillouin-zone LBM predictions to be the most accurate, as this method makes the least assumptions regarding the nature of phonon transport. We will use the full Brillouin-zone results to assess the suitability of the simplified models described in Secs. III B–III D.

The per-phonon mode thermal conductivity contribution for bulk SW silicon and the 17.4 nm thin film are plotted versus the bulk MFP in Fig. 5(a). Similar plots for larger film thicknesses show a smooth transition to the bulk behavior. Since our model systems contain no defects, no free electrons, and no internal interfaces, the large MFPs presented in Fig. 5(a) are not surprising. A real silicon sample, which includes these additional phonon scattering mechanisms, will have smaller MFPs and the thin film thermal conductivity would approach the bulk value at a smaller length scale than observed in Fig. 4. For bulk SW silicon at a temperature of 300 K, phonons with MFPs larger than 1 μm contribute 44% of the total thermal conductivity. This value is consistent with that found by Henry and Chen,³³ who used MD

TABLE I. Thermal conductivity predictions for bulk SW silicon and thin films (cross-plane direction) at a temperature of 300 K.

Length, L_z (nm)	Thermal conductivity, k_z (W/m K)			
	Full Brillouin- zone	Isotropic approximation	Gray approximation	Matthiessen rule
17.4	10.5	8.5	14.4	10.4
100	67.9	53.1	115	67.8
1000	236	180	407	235
5000	419	334	553	418
Bulk	574	489	N/A	N/A

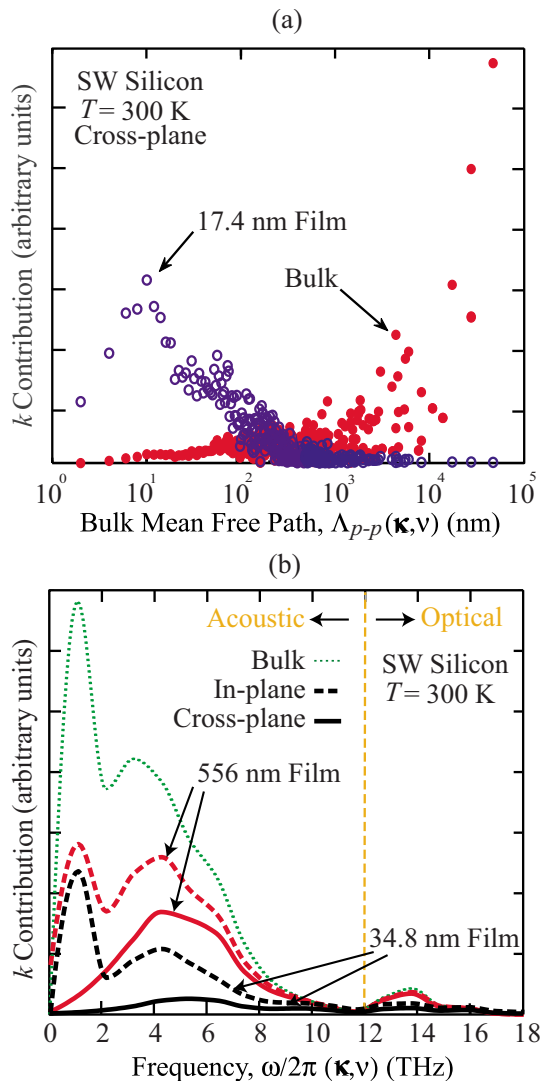


FIG. 5. (Color online) (a) Cross-plane thermal conductivity contribution dependence on the bulk phonon MFP. The MFPs for each mode are sorted using a histogram with a bin width of 2 nm. The thermal conductivity contribution is normalized by the total value. (b) Thermal conductivity contribution dependence on frequency for bulk and for 556 and 34.8 nm thin films. The area under each curve is proportional to the total thermal conductivity. The in-plane data are from Ref. 5.

simulation and normal mode analysis^{8,9} to predict their phonon properties. As the film thickness is reduced, boundary scattering becomes important and the effective MFPs of these modes are reduced to the system size and they contribute less to thermal conductivity.

The frequency-dependent contribution to the thermal conductivity of bulk SW silicon and the cross-plane and in-plane orientations for the 556 and 34.8 nm thin films is plotted in Fig. 5(b).³⁴ The area under each curve is proportional to the total thermal conductivity. For bulk SW silicon, the thermal conductivity is dominated by large-MFP acoustic phonons with frequencies less than 2 THz, where the slopes of the dispersion curves are the steepest [corresponding to large group velocities, see Fig. 3(a)] and the relaxation times are large [see Fig. 3(b)].

The in-plane thermal conductivity is higher than the cross-plane value for all film thicknesses. The phonons that travel parallel (or close to parallel) to the system boundaries

contribute significantly to the in-plane thermal conductivity and are not hindered (or only slightly hindered) by the system boundaries. Therefore, the large-MFP phonons with frequencies less than 2 THz that dominate the bulk thermal conductivity also dominate the in-plane thermal conductivity. The phonons traveling perpendicular (or close to perpendicular) to the system boundaries, however, are significantly impeded by the boundaries and thus have reduced cross-plane MFPs. Therefore, the cross-plane thermal conductivity is lower than the in-plane value. Since the cross-plane MFPs are reduced to the system length, the phonons with frequencies less than 2 THz do not contribute significantly to thermal transport because they have a small density of states.³⁵ The cross-plane thermal conductivity is thus dominated by midfrequency phonons, which, while having smaller bulk MFPs, have a large density of states.

It is often assumed that optical phonons ($\omega > 12$ THz for SW silicon) do not contribute significantly to bulk thermal conductivity due to their small MFPs. We find that optical phonons contribute 3.5% to the thermal conductivity of bulk SW silicon. Neglecting their thermal conductivity contribution is therefore not unreasonable, although their effect on scattering must be included in the calculation of $\tau_{p-p}(\boldsymbol{\kappa}, \nu)$ (Ref. 24). As the film thickness is reduced, however, the relative contribution of these small MFP modes increases. For the smallest film investigated ($L_z = 17.4$ nm), optical modes contribute 22.5% to the cross-plane thermal conductivity. For the in-plane orientation, the increase is not as significant (a maximum contribution of 8% for the 17.4 nm film).

B. Isotropic approximation

To simplify the prediction of thermal conductivity, it is convenient to assume that the material of interest is isotropic (i.e., the crystal is uniform in all directions). The bulk thermal conductivity calculated using the isotropic approximation and the phonon properties along the [001] direction is 489 W/m K, which is within 15% of the bulk thermal conductivity predicted using all of the phonons in the Brillouin-zone, 574 W/m K. To understand this reasonable agreement, given the reduction in LBM computational cost (by three orders of magnitude), consider the dispersion data and relaxation times plotted in Figs. 3(a) and 3(b). The frequencies show a strong isotropic trend near the Brillouin-zone center. The group velocities, which are the derivatives of the frequencies with respect to the wave vector magnitudes, will also exhibit a similar trend. The relaxation times are also reasonably isotropic in nature (i.e., a function of frequency only) and near the Brillouin-zone center, they collapse onto a single curve that is well represented by the $\tau = A/\omega^2$ relationship proposed by Callaway.³⁶ Since bulk thermal conductivity is dominated by phonons that are located near the Brillouin-zone center [see Fig. 5(b)], it is not surprising that the isotropic approximation is reasonable for bulk SW silicon.

The suitability of the isotropic approximation for bulk SW silicon contrasts the behavior of Lennard-Jones (LJ) argon, where Turney *et al.*⁷ found, using MD simulation and

normal mode analysis, that the isotropic approximation under-predicts the bulk thermal conductivity by a factor of 1.5 at a temperature of 40 K (about half the LJ argon melting temperature). They explain their finding by noting that the largest contribution to LJ argon bulk thermal conductivity comes from phonons around half of the maximum frequency, where group velocities in the [001] direction are not representative of the entire Brillouin-zone.

When the LBM is used to evaluate the cross-plane thin film thermal conductivities, the difference between the isotropic and full Brillouin-zone predictions increases from 15% for a bulk system to 25% for the 17.4 nm film. As the film thickness is reduced, the contribution of the higher frequency modes becomes increasingly important [see Fig. 5(b)]. Because the group velocities corresponding to the full Brillouin-zone deviate from the [001] behavior for these phonons [see Fig. 3(a)], the isotropic approximation becomes increasingly less accurate as film thickness is reduced.

C. Simplified model based on the Gray approximation

Previous works have used models based on an averaged, single bulk MFP, Λ_{Bulk} , (i.e., the Gray approximation) for predicting the thermal conductivity reduction in thin films.^{20,37} Using our lattice dynamics results, we compute Λ_{Bulk} from

$$\Lambda_{\text{Bulk}} = \frac{k_z}{\sum_{\nu} \sum_{\boldsymbol{\kappa}} c_{ph}(\boldsymbol{\kappa}, \nu) |v_{g,z}(\boldsymbol{\kappa}, \nu)|}, \quad (13)$$

giving 246 nm for SW silicon at a temperature of 300 K. In Fig. 4 we use this value in a simplified model developed by Majumdar,²⁰

$$\frac{k_{\text{Film}}}{k_{\text{Bulk}}} = \frac{1}{1 + 4\Lambda_{\text{Bulk}}/3L_z}, \quad (14)$$

to predict the cross-plane thermal conductivity. This model, which was developed using the equation of phonon radiative transfer and diffuse boundary conditions, does not capture the correct convergence to the bulk thermal conductivity and over-predicts the full Brillouin-zone values (by as much as 81% at $L_z = 500$ nm). Turney *et al.*⁵ report that similar models developed for the in-plane direction^{20,37} also do not accurately capture the thermal conductivity reduction. For confined thin films, Landry and McGaughey³⁵ found that a single MFP cannot be used to describe the cross-plane phonon transport.

D. Boundary scattering and the Matthiessen rule

To include boundary scattering in thermal conductivity predictions using Eq. (7), we use the Matthiessen rule. The Matthiessen rule combines the relaxation times of different scattering mechanisms by assuming them to be independent. This assumption was shown by Turney *et al.* to introduce at most 12% error for in-plane phonon transport.⁵ We use the Matthiessen rule to combine the phonon-boundary scattering

relaxation times, $\tau_b(\boldsymbol{\kappa}, \nu)$, with the intrinsic phonon-phonon relaxation times obtained from lattice dynamics calculations, $\tau_{p-p}(\boldsymbol{\kappa}, \nu)$, to give an effective relaxation time, $\tau_M(\boldsymbol{\kappa}, \nu)$ (Refs. 12 and 22)

$$\frac{1}{\tau_M(\boldsymbol{\kappa}, \nu)} = \frac{1}{\tau_{p-p}(\boldsymbol{\kappa}, \nu)} + \frac{1}{\tau_b(\boldsymbol{\kappa}, \nu)}. \quad (15)$$

We take the boundary scattering relaxation time to be equal to the average time between boundary scattering events in the absence of intrinsic scattering, i.e.,^{5,38}

$$\tau_b(\boldsymbol{\kappa}, \nu) = \frac{L_z}{2|v_{g,\zeta}(\boldsymbol{\kappa}, \nu)|}. \quad (16)$$

In Fig. 4 and Table I, the cross-plane thermal conductivities predicted using Eq. (7) with Eqs. (15) and (16) are presented with the results obtained using the LBM. In the LBM, the phonon-phonon scattering and phonon-boundary scattering are treated independently. Since the Matthiessen rule also assumes that the scattering mechanisms are independent, agreement between the two methods is expected, provided that the boundary scattering is correctly modeled. The agreement with the LBM (within 1% for all film thicknesses) suggests that Eq. (16) is appropriate for modeling diffuse boundaries.

Using the lattice dynamics-predicted phonon properties to calculate the cross-plane thermal conductivity with the Matthiessen rule and Eq. (7) is less computationally expensive than using the LBM procedure (i.e., seconds to generate a solution for a 5 μm film compared to days for the LBM). Thus, if only the thermal conductivity is required, we suggest using the Matthiessen rule and Eq. (7). However, if the occupation numbers or the temperature profile are required, the LBM procedure should be used.

IV. SUMMARY

We used a hierarchical method that considers all of the phonons in the first Brillouin-zone to predict the cross-plane thermal conductivity of SW silicon thin films. We analyzed the in-plane orientation in a previous report⁵ and find that the cross-plane thermal conductivity is less than the in-plane value for all film thicknesses. Our cross-plane thin film thermal conductivity predictions are in excellent agreement with those predicted using the Matthiessen rule to incorporate boundary scattering (Sec. III D).

Considering all of the phonons in the first Brillouin-zone allowed us to examine common assumptions used to reduce the computational effort. Because the frequency dependence of thermal conductivity changes as film thickness is reduced [see Fig. 5(b)], assumptions that are valid for bulk are not necessarily valid for thin films. This trend is most evident for the contribution of optical phonon modes. For bulk SW silicon, optical modes contribute 3.5% to the total thermal conductivity and neglecting their contribution is reasonable. For the thin films, however, neglecting optical modes can introduce sizable error (up to 22.5% for the 17.4 nm film).

By examining the phonon dispersion data and relaxation times in Figs. 3(a) and 3(b), we showed that the phonons along the [001] direction are representative of the full

Brillouin-zone data at low-frequencies. Since the bulk thermal conductivity of SW silicon is dominated by low-frequency phonons, the isotropic approximations yields bulk thermal conductivity predictions that are within 15% of the true value. Because the cross-plane contribution of these low-frequency phonons is reduced as the film thickness is reduced, however, the isotropic approximation introduces up to 25% error when modeling the thin films. Error is also introduced when an averaged, bulk MFP is used to predict the thermal conductivity reduction in thin films (Sec. III C).

The usefulness of our hierarchical method lies in its generality. Although used here to predict the cross-plane thermal conductivity of SW silicon thin films, this method can be extended to describe the transient phonon behavior in any crystalline material, provided the force constants required as input to the lattice dynamics calculations can be obtained. If these force constants can be calculated using quantum calculations, such as density functional theory,²⁴ the hierarchical method will provide an efficient means for modeling transient phonon transport from first principles.

ACKNOWLEDGMENTS

We acknowledge support from the Natural Sciences and Engineering Research Council of Canada and Advanced Micro Devices. We thank E. S. Landry (Lytron, Inc.), J. A. Thomas (Johns Hopkins University Applied Physics Laboratory), and A. Nabovati (University of Toronto) for providing suggestions to improve the manuscript.

- ¹D. G. Cahill, K. E. Goodson, and A. Majumdar, *J. Heat Transfer* **124**, 223 (2002).
- ²D. G. Cahill, W. K. Ford, K. E. Goodson, G. D. Mahan, A. Majumdar, H. J. Maris, R. Merlin, and S. R. Phillpot, *J. Appl. Phys.* **93**, 793 (2003).
- ³E. Pop and K. E. Goodson, *J. Electron. Packag.* **128**, 102 (2006).
- ⁴A. D. McConnell and K. E. Goodson, *Annu. Rev. Heat Transfer* **14**, 129 (2005).
- ⁵J. E. Turney, A. J. H. McGaughey, and C. H. Amon, *J. Appl. Phys.* **107**, 024317 (2010).
- ⁶M. T. Dove, *Introduction to Lattice Dynamics* (Cambridge University Press, Cambridge, 1993).
- ⁷J. E. Turney, E. S. Landry, A. J. H. McGaughey, and C. H. Amon, *Phys. Rev. B* **79**, 064301 (2009).
- ⁸A. J. C. Ladd, B. Moran, and W. G. Hoover, *Phys. Rev. B* **34**, 5058 (1986).
- ⁹A. J. H. McGaughey and M. Kaviany, *Phys. Rev. B* **69**, 094303 (2004).
- ¹⁰A. A. Maradudin and A. E. Fein, *Phys. Rev.* **128**, 2589 (1962).
- ¹¹D. A. Broido, A. Ward, and N. Mingo, *Phys. Rev. B* **72**, 014308 (2005).
- ¹²G. P. Srivastava, *The Physics of Phonons* (Adam Hilger, Bristol, 1990).
- ¹³R. A. Escobar, S. S. Ghai, M. S. Jhon, and C. Amon, *Int. J. Heat Mass Transfer* **49**, 97 (2006).
- ¹⁴R. A. Guyer, *Phys. Rev. E* **50**, 4596 (1994).
- ¹⁵R. A. Escobar, B. Smith, and C. H. Amon, *J. Electron. Packag.* **128**, 115 (2006).
- ¹⁶W.-S. Jiaung and J.-R. Ho, *Phys. Rev. E* **77**, 066710 (2008).
- ¹⁷P. Heino, *Comput. Math. Appl.* **59**, 2351 (2010).
- ¹⁸A. Christensen and S. Graham, *Numer. Heat Transfer* **57**, 102401 (2010).
- ¹⁹J. V. Goicochea, M. Madrid, and C. H. Amon, *J. Heat Transfer* **132**, 89 (2010).
- ²⁰A. Majumdar, *J. Heat Transfer* **115**, 7 (1993).
- ²¹M. F. Modest, *Radiative Heat Transfer* (McGraw-Hill, New York, 1993).
- ²²J. M. Ziman, *Electrons and Phonons* (Oxford University Press, New York, 2001).
- ²³M. Omini and A. Sparavigna, *Phys. Rev. B* **53**, 9064 (1996).
- ²⁴A. Ward and D. A. Broido, *Phys. Rev. B* **81**, 085205 (2010).
- ²⁵M. Omini and A. Sparavigna, *Philos. Mag. B* **68**, 767 (1993).
- ²⁶D. A. Broido and T. L. Reinecke, *Phys. Rev. B* **51**, 13797 (1995).

- ²⁷N. W. Ashcroft and N. D. Mermin, *Solid State Physics* (Sauders College, Fort Worth, 1976).
- ²⁸A. Nabovati, D. P. Sellan, and C. H. Amon (unpublished).
- ²⁹J. V. Goicochea, Ph.D. thesis, Carnegie Mellon University, 2008.
- ³⁰E. S. Landry and A. J. H. McGaughey, *Phys. Rev. B* **79**, 075316 (2009).
- ³¹J. E. Turney, A. J. H. McGaughey, and C. H. Amon, *Phys. Rev. B* **79**, 224305 (2009).
- ³²D. G. Cahill and F. Watanabe, *Phys. Rev. B* **70**, 235322 (2004).
- ³³A. S. Henry and G. Chen, *J. Comput. Theor. Nanosci.* **5**, 2 (2008).
- ³⁴The in-plane values were calculated by Turney *et al.*⁵ using a BTE/ Matthiessen rule-based procedure that considers diffuse boundaries. For consistency, the cross-plane data in Fig. 5(b) are also calculated using the Matthiessen rule (see Sec. III D).
- ³⁵E. S. Landry and A. J. H. McGaughey, *J. Appl. Phys.* **107**, 013521 (2010).
- ³⁶J. Callaway, *Phys. Rev.* **113**, 1046 (1959).
- ³⁷M. Flik and C. Tien, *J. Heat Transfer* **112**, 872 (1990).
- ³⁸D. P. Sellan, E. S. Landry, J. E. Turney, A. J. H. McGaughey, and C. H. Amon, *Phys. Rev. B* **81**, 214305 (2010).